RSC Advances

ROYAL SOCIETY OF CHEMISTRY

www.rsc.org/advances

Journal Name

RSCPublishing

ARTICLE

NXO Beta Structure Mimicry: An Ultrashort Turn/ Hairpin Mimic that Folds in Water

Cite this: DOI: 10.1039/x0xx00000x

Constantin Rabong,[b] Christoph Schuster,[c] Tibor Liptaj,[d] Nadežda Prónayová,[d] Vassil B. Delchev,[e] Ulrich Jordis,[b] and Jaywant Phopase*[a]

Received 00th January 2012,
Accepted 00th January 2012

DOI: 10.1039/x0xx00000x

www.rsc.org/

We report the first application of NXO-pseudopeptides for β-turn mimicry. Incorporating the proline-derived NProO peptidomimetic building block, a minimal tetrapeptide β-hairpin mimic has been designed, synthesized and its solution structure elucidated. Emulating a natural proline-glycine β-turn, evidence from NMR, molecular modeling and CD suggests the formation of two rapidly interconverting hairpin folds in water, methanol and dimethylsulfoxide at room temperature, displaying the proline nitrogen amide bond in either *cis* or *trans* arrangement. The NProO-modified hairpin features peptidic backbone dihedrals Φ, Ψ characteristic of natural proline-containing turns composed of α-amino-acids only. Taken together, the observed folding behavior and inherently high designability render the NProO motif a building block for β-structure elaboration in aqueous medium.

1 Introduction

For a long time, peptidomimetics with predictable secondary structure characteristics have been in high demand in medicinally oriented synthetic chemistry.[1] Combinatorial accessibility, straightforward synthetic diversification and stereochemical integrity during all manipulations are some of their prime features. In principle, all β-secondary structure mimicry relies on a turn-inducing motif with adjacent strands. Any turn mimic must, while suitably orienting the strand backbones to each other, arrange reversal in peptide backbone direction. However, it has been recognized that amino acid side chain functionalities contribute to the stability of the generated fold, as well.[2] Here, the intrinsic secondary structure propensities of sequenced amino acids and their cross-strand pairing propensities are the principal influences governing the native state ensemble.[3]

The NXO concept represents an undertaking to create a synthetic foldamer scaffold amenable to elaboration of secondary structure found in peptides, in particular β-structure.[4] Incorporating structure-guiding motifs at the repeating unit level, NXO-peptides mimic the dipole polarization of a natural amino acid backbone in β-sheet configuration (Fig. 1). Self-organizing within a mutually attractive hydrogen bonding pattern, NXO-modified peptides adopt extended folds.[5] By virtue of their conformationally biased hydrazide (-NH-NH-CO-) "N"- and oxalamide (-CO-CO-NH-) "O"-retrons, NXO-modified peptides sample the characteristic "X" amino acid dihedral angles Φ and Ψ in conformational space characteristic of β-structure.[6]

Selective restriction of conformational freedom and hence limitation of accessible molecular phase space has been a guiding theme in the development of new peptidomimetic scaffolds.[1a-d] Relying conceptionally on a restrained (often cyclic) turn-inducing template motif predisposing attractive strand-strand interactions, ingenious and sophisticated technologies have emerged.[7] Enabling synthetic access to an ever-increasing number of peptide and foldamer sequences predictably adopting β-structure, the study of conformationally constrained peptidomimetics has been essential for an understanding of the principles underlying the generation of structure from sequence in natural proteins. Still, crafting a peptidomimetic foldamer intended for directed self-assembly in aqueous medium remains a daunting challenge.[8]

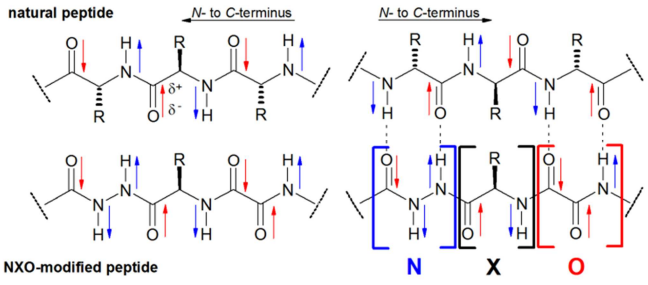

Fig. 1 Left: Comparison of the backbone donor-acceptor dipole pattern in a natural peptide with NXO-modified peptides. The arrows near CO- and NH-bonds depict the orientation of the local dipole. Right: Matching hydrogen bond donor and acceptor groups allow NXO-modified peptides to interact with natural peptides. R = amino acid side chain, X = any amino acid.

At first sight, hydrogen bonding may not seem to be the top choice non-covalent interaction to stabilize secondary structure in the design of small molecule topomimetics.[9] The main shortcomings of hydrogen bonds regarding technological exploitation as structure-guiding motifs are their intrinsic kinetic liability and reversibility of association. In protein β-sheets, cross-strand hydrogen bonding contributes most favorably when located in a hydrophobic region of the folded structure.[10] However, the backbone of a small peptidomimetic must be regarded

as virtually completely solvent exposed.[11] A polar, protic medium like water will therefore effectively compete for hydrogen bonding interactions and relatively diminish intramolecular association. Notwithstanding, there are unique assets of hydrogen bonds: They are sequence-unspecific and feature strongly directional geometric restraints.

This paper describes the design, synthesis and analysis of a minimal β-turn mimic incorporating the L-proline derived NProO modification. We report our efforts towards expanding the frontiers in β-structure mimicry: Investigating peptidomimetic secondary structure motif-guided self-assembly in water at room temperature while, in an anticipated extension towards NXO-modified β-sheets, rendering the turn site functionally designable.[12]

2 Results and discussion

2.1 Design and Synthesis of an NXO β-turn/hairpin-mimic

Reverse turns are sites where the protein chain changes its direction, a prerequisite for the close packing seen in globular proteins. Often located at solvent-exposed protein surfaces, a good deal of molecular recognition and protein host-guest events known today are taking place here. Hence, a designable turn/hairpin peptidomimetic can be most useful.[13] In proteins, proline is found at around 30% of turn *i*+1 positions.[14] The design prerequisite of maintaining close topological analogy to the majority of L-proline containing turn sites of natural origin[15] and previous studies[16] motivated us to examine the turn-inducing capability of NXO-modified proline in the context of the extensively probed and proven two-residue proline-glycine turn scaffold (Fig. 2).[17] We sought to mimic hairpin folding of a natural tetrapeptide sequence featuring an NXO-modified turn with L-proline at *i*+1.[18] Incorporating the L-proline-derived N^{L}ProO building block, the natural sequence would be modified accordingly: At the peptidic *C*-end, we introduced the conformationally more flexible, stronger solvent interacting hydrazide "N"-retron[19] to mimic the turn glycine at *i*+2 whereas the *anti*-restrained oxalamide[20] "O"-retron would constitute the *i*-position *N*-terminal.

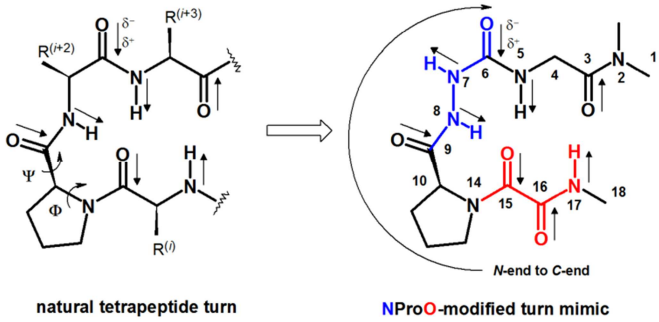

Fig. 2 Design rational for NProO-modified β-turn/hairpin mimic incorporating L-proline-glycine turn. Arrows next to bonds show the direction of the local dipole. Atom numbering given as used throughout the text.

Aiming to investigate the conformation of NXO-modified proline in water, β-turn mimic **1** was designed (Fig. 2). In order to maintain the structural topology of the β-turn a urea motif was chosen as a linker between the N^{L}ProO hydrazide terminal at *i*+2 and *i*+3 glycine. Dimethylamino and methylamino functions were used for endcapping of the C- and N-terminals, respectively.

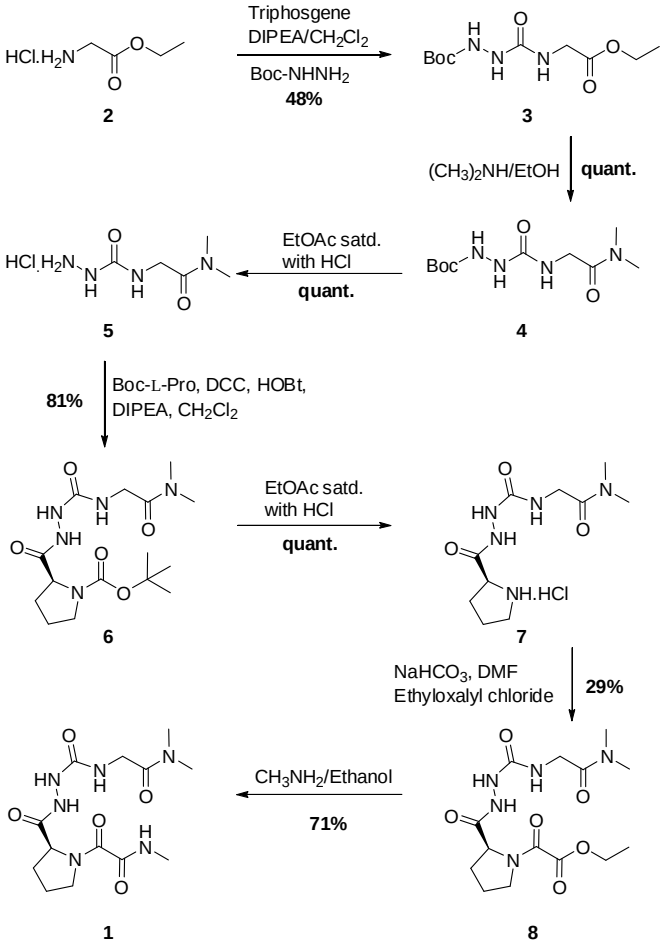

Scheme 1 Synthesis of N^{L}ProO-modified β-turn mimic **1**.

β-turn **1** was prepared starting from commercially available glycine ethyl ester hydrochloride **2** (Scheme 1). **2** was reacted with phosgene in the presence of DIPEA (ethyldiisopropylamine) in dichloromethane to generate the corresponding isocyanate in situ, which was further reacted with Boc-hydrazide to give **3** in 48% overall yield. Compound **4** was generated in quantitative yield via direct amidation of ethyl ester **3** with dimethylamine in ethanol. Boc-deprotection by treatment of **4** with HCl-saturated ethyl acetate gave the product as the corresponding hydrochloride **5** in quantitative yield. **7** was prepared in two steps from **5**: Firstly, **5** was reacted with Boc-L-proline using DCC (*N*,*N*'-dicyclohexylcarbodiimide) and HOBt (1-hydroxybenzotriazole) as coupling agents and DIPEA as base in dichloromethane to give **6** in 81% yield. Boc-deprotection using HCl-saturated ethyl acetate afforded **7** in quantitative yield. Compound **8** was found elusive towards isolation and attempts to react with oxalylchloride monoethyl or monomethyl ester using organic auxiliary bases (DIPEA, triethylamine) generated inseparable mixtures. Ultimately, **8** was prepared using a previously optimized protocol where **7** was treated with ethyl oxalylchloride in the presence of sodium bicarbonate in DMF at 0°C, affording crude **8** in 29% yield.[4b] Without further purification, **8** was immediately reacted with a solution of methylamine in ethanol to afford **1** in 71% yield.

2.2 Conformation analysis of 1 by stochastic conformational searching and solution phase Molecular Dynamics (MD) studies

Minimum energy conformation analysis and MD (Molecular Dynamics) were undertaken to assess folding and ensemble stability of **1**.[21] Stochastic conformation searching of $>10^6$ ROESY (rotating-frame nuclear Overhauser effect correlation spectroscopy)-restrained, OPLS-AA-derived[22] input geometries generated 956 conformations of which the 10 energy-lowest are shown RMSD (root-mean-square deviation)-superposed in Fig. 3, left model. All conformations are sampled in a reverse-turn characterized by hydrogen bond formation between acceptors and donors at (C3)O←HN17 and (C15)O←HN5, with (C15)O ←HN8 providing additional stabilization. The interstrand distance C4-C16 (corresponding to Pos. *i* and *i*+3) measuring on average 5.4±0.5Å, **1** adopts a β-hairpin with a ten-membered β-turn.[23] With the configuration of the turn-site proline given in the N^{L}ProO-modification, the (C15)O←HN8 bonding motif can be formally assigned to be part of an inverse γ-turn,[24] found frequently at the loop end in protein β-sheets.[25]

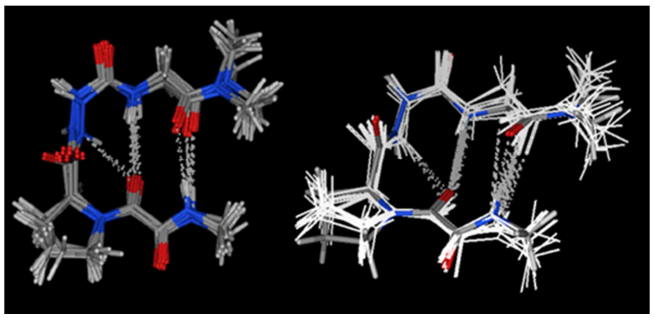

Fig. 3 Molecular modeling of **1**. Left: The ten energy-lowest geometries from a ROESY-restrained stochastic search within the OPLS-AA forcefield, spanning a range of 8.2kcalmol^{-1}, are shown superposed. Right: The minimum energy geometry from stochastic searching (colored model) superposed with the core RMSD (ΔRMSD= 1.06±0.09Å) region sampled during a 100ns MD run in water at 290K (white models). Dotted lines indicate hydrogen bonding.

The lowest energy conformer generated was then freed of restraints and input to MD simulations with OPLS-AA parameters and implicitly treated solute-solvent interactions (Generalized Born model of solvation). The calculated trajectories further sustain the evidence that turn-site (*i*+1, *i*+2)-N^{L}ProO incorporation stabilizes a hairpin conformation in a tetrapeptide mimicking sequence (Fig. 3, right model).[26] 100ns trajectories in DMSO (medium relative permittivity ε=47Debye) at 297K and 327K display **1** as a β-turn adopting hairpin fold (see Fig. 2-4 and Table 2, supplementary information) in rapid equilibrium with an extended conformation throughout the entire simulation time. Again, the fold is mainly stabilized by dual hydrogen bonding at (C15)O←HN5 and (C3)O←HN17, with additional contributions stemming from (C15)O←HN8. 100ns MD simulations in water (ε=78.5Debye) give a qualitatively similar picture, that is, calculations do not show increased medium polarity detrimentally impacting the folding ability via destabilization of interstrand hydrogen bonding. The average hydrogen bonding lifetimes (see Table 3, supplementary information) are seen similar in both media, with (C3)O←HN17 and (C15)O←HN8, (C15)O←HN5 around 2.8ps and 2.1ps, respectively. Peptide backbone dihedrals representing the NXO-modified turn site in **1** are displayed in the same regions of the Ramachandran plot also populated by natural peptides composed of α-amino acids.[27] N^{L}ProO at *i*+1 exhibits Φ (C15-N14-C10-C9; histogram data (see Fig. 5, supplementary information) around -72±8° while displaying two significant maxima for Ψ (N14-C10-C9-N8) at +109±18° and +154±20°, thus within the core β-region and characteristic of L-proline at *i*+1 in a turn configuration.[28] MD simulation gives the *i*-position "O"-oxalamide constrained to *ap* (antiperiplanar) around 0(180)°. The NXO-modified hydrazide glycine at *i*+2 exhibits pertinent backbone dihedrals, sampling Φ (C9-N8-C7-C6) at +102±18 and -111 ±15° and Ψ (N8-N7-C6-N5) at 0(180) ±8°, mimicking glycine at *i*+2 in backbones consisting of α-amino acids.[29] From MD simulations, N7H is seen pointing out of the turn cavity in the folded state. Instructively, facile rotation around the N8-N7-axis in the "N"-hydrazide motif, not attainable in the folded conformation, occurs in the extended conformation and during un- and refolding; H-N7-N8-H is displayed at +106 ±24°.[30] Here, N8H is seen to provide crucial hydrogen bond donor capacity (H-N8-C9-C10 around +170±11°), acting as a nucleation site for folding. Hierarchically, after the innermost hydrogen bond (C15)O←HN8 is transiently established during incipient folding,[31] association via interstand binding (C15)O←HN5 sets the stage for establishing the prevailing hairpin conformation.[32]

2.3 NMR analysis of 1

Owing to the poor solubility of **1** in nonpolar solvents, NMR-experiments had to be restricted to water (H_2O:D_2O =9:1), DMSO-d_6 and MeOH-d_4. In DMSO-d_6, a first clue towards hydrogen bonding as a main factor contributing to fold stabilization were the shifts of the C5-urea and C17-oxalamide NH-signals appearing at δ=6.30ppm and 8.68ppm respectively, both well downfield from their resonances (δ~4.5 and 7.5ppm respectively) under conditions where no hydrogen bonding occurs.[33] Given the observed chemical shift invariability upon varying sample concentration (between 2.5 to 25mM), this interaction was concluded to be intramolecular. In water, a fast exchange of NH protons with the solvent was seen; yet, N5H was observable even upon 1.5s of water presaturation in the DPFGSE-NOE (double pulsed field gradient spin echo-nuclear Overhauser effect spectroscopy) experiment,[34] again likely so due to intramolecular hydrogen bonding.[35]

All experiments generated two distinctly different sets of signals in a ratio of ~3:2 (by integration of the respective C1 and C18 signals, see Fig. 4). Investigating the constitutional identity of these two species with COSY (correlation spectroscopy) and TOCSY (total correlation spectroscopy) experiments, their atom-connectivities were found similar; assignment of conformations was next to tackle. Bearing in mind the well described but generally slow *cis-trans* isomerism of *N*-substituted prolines, we first envisaged a diasteromeric pair of N14-C15 amide rotamers.[36] Given that shift differences between the two signal sets decreased proceeding towards the end of both strands from the proline ring onward (by up to 0.6ppm for C10H, resonating at δ=4.94ppm and 4.34ppm in the major and minor set in DMSO-d_6, respectively), we concluded magnetic anisotropy around the stereogenic proline carbon to be the likely cause of splitting. That the two experimentally observed signal sets corresponded to the open and folded conformers seen in MD simulations (see Fig. 3, supplementary information) was excluded: Firstly, both observed sets displayed signals characteristic of geometries with restricted backbone rotations. Secondly, the open-fold interconversion rate was simulated in

the order of magnitude of 10^{-11}s at 290K, too fast to be discernable by the NMR experiments undertaken.

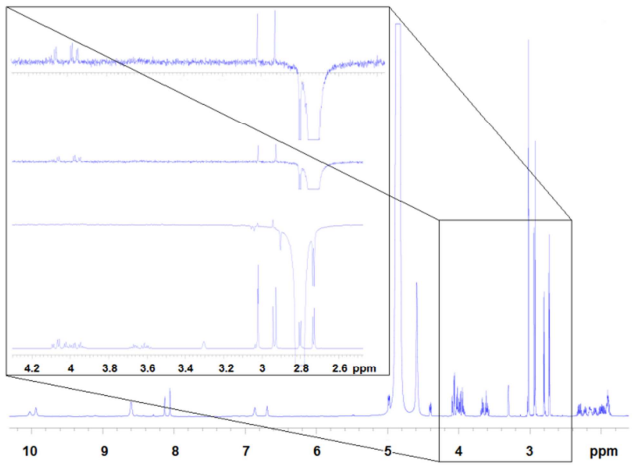

Fig. 4 600 MHz ^{1}H NMR spectrum of **1** in MeOH-d_4 (298K, 5mM). Displayed in the box is the selective DPFGSE-NOE irradiation of the C18 methyl group protons in both species **1a** and **1b** (at δ=2.80ppm and 2.73ppm), showing NOE enhancement of the C1 methyl signals at δ=2.93ppm and 3.02ppm, respectively.

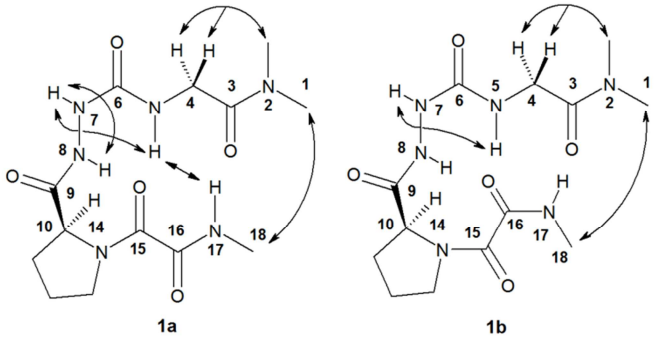

Fig. 5 Key NOE interactions in **1**, shown for both observed equilibrium geometries **1a** and **1b**. NOESY was carried out with a mixing time of 250ms at 290K, 297K and 298K in H_2O:D_2O=9:1, DMSO-d_6 and MeOH-d_4, respectively, at 5mM concentration.

Observing NOE (nuclear Overhauser effect spectroscopy) enhancements of methyloxalamide C18H and dimethylamide C1H (Fig. 4 and 5) in both species, conformations with spatial proximity of strand-ends were indicated. Thus, the existence of two different sets of signals had to be explained in terms of two folds, rapidly equilibrating at NMR timescale.

Among envisaged structures were isomers exhibiting either a C9-C10 *cis*-amide or C15-C16 *cis*-oxalyl unit. Further, a *cis*-proline (N14-C15) conformer was contemplated, yet it remained unclear how such a fold would realize across-strand hydrogen bonding (experimentally indicated, though, by the downfield-shifting of the amide protons N5H and N17H observed in both signal sets). Ultimately, *ab initio* quantum mechanical calculation of NMR chemical shifts at the B3LYP/6-311G++(d,p) level of theory, including implicit solvation, clarified the issue: Among the minimum energy geometries located and substantiated by comparison to MD trajectories (see chapter 2.2), next to the previously observed hairpin (**1a**, Fig. 5, left structure and Fig. 6, blue model), a minimum geometry exhibiting the conspicuous downfield chemical shift of C10H was calculated (**1b**, Fig. 5, right structure and Fig. 6, red model). Overall in good agreement with experimental proton chemical shifts (Fig. 6 and 7, supplemantary information), this geometry displayed both the amide linkage at the proline nitrogen and the strand-terminating methyl oxalamide unit in *cis*-arrangement.[37] According to calculations, geometry **1b** is 0.05-0.22kcalmol^{-1} more stable than **1a**. Although in isomer **1b** the proline amide bond N14-C15 is in *cis* arrangement,[38] concomitant rotation in the C16-N17 methylamide subunit allows **1b** to project the terminal methyl C18 spatially similar to **1a** while engaging in interstrand hydrogen bonding.

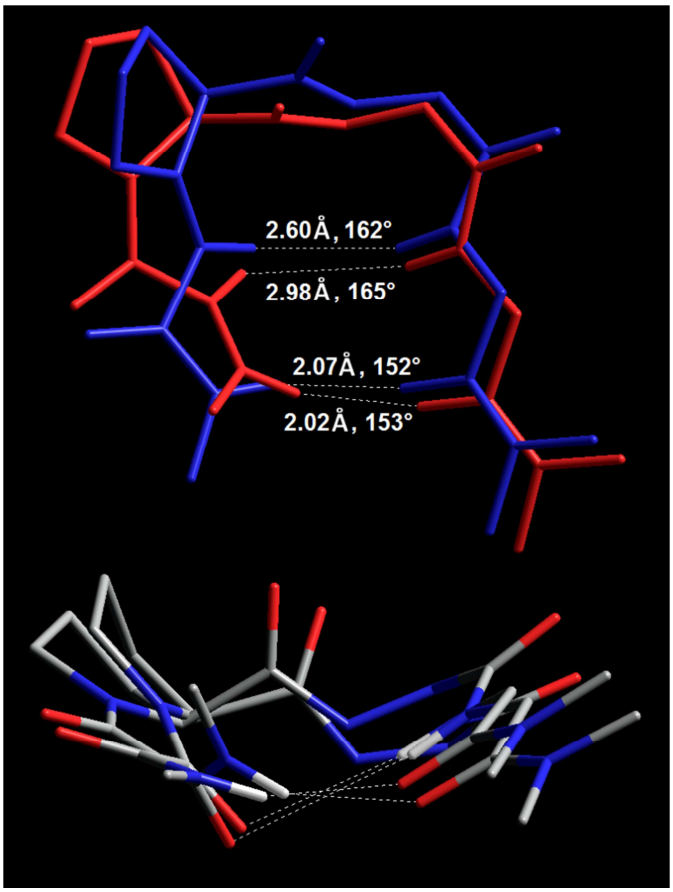

Fig. 6 All-atom RMSD-minimized superposition of the two main conformers of **1**, calculated by *ab initio* methods and supported by NMR and MD. In the top model overlay, the geometries of conformers **1a** and **1b** are blue and red respectively; ΔRMSD (all atoms) is 1.20Å. Dotted lines indicate hydrogen bonds, with calculated distances and angles (O-H-N) given in the figure. Non-interacting hydrogens omitted for clarity.

2.4 Studies of 1 by Circular Dichroism

While a delicate probe to study molecular conformation, CD (circular dichroism) cannot necessarily induce the structure characteristics of foldamers featuring novel functionalities.[39] As a reference and conceptual augmentation, we prepared the N^{D}ProO-derivative **9**, the enantiomer of **1**, incorporating D-proline. The measurements shown in Fig. 7 provide evidence corroborating positive formation of a distinctive molecular conformation. In all three solvents of examination, **1** and **9** exhibit graphs characteristic of β-secondary structure: Indicating β-turn adoption in water, **1** shows ellipticity θ maximal at λ=231nm and a zero-transition at 209nm, relatively red-shifted to the CD

values for natural β-sheets.[40] Folding propensities, taken from θ at 190nm and from the local maxima in the 230-240nm region, diminish on going from acetonitrile to methanol and water, correlating with solvent polarity. Thus, in agreement with NMR experiments, folding to a central well-defined spatial motif was observed in polar protic and aprotic medium alike.

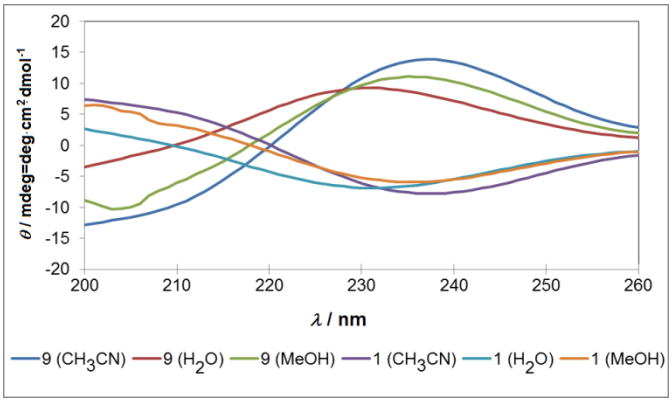

Fig. 7 CD graphs of **1** and corresponding D-proline enantiomer **9** in acetonitrile, methanol and water. Measurements were carried out at 295K and 0.1mM concentration.

2.5 Discussion

The studies undertaken in the context of this work present the N^{L}ProO-modified model peptidomimetic **1** folding to a minimal β -sheet increment, displaying the aptitude of NXO-modified peptides to engage extensively in intrastrand hydrogen bonding. Subordinate to a fast (in the order of magnitude of 10^{-11}s at 290 K) open-fold equilibrium, **1** adopts a native state of two β-turn conformers in aqueous medium around room temperature: The *trans*-proline hairpin **1a** and the *cis*-proline conformer **1b**, the latter being slightly more abundant (ratio **1a**:**1b**~2:3) and exhibitting a *cis*-proline amide bond and a *cis*-oxalyl unit in the oxalamide "O"-motif. **1a** and **1b** feature dual interstrand hydrogen bonding interactions. Shown in Fig. 8 are backbone-RMSD minimized overlays of the β-hairpin equilibrium geometry **1a**, supported by spectroscopy and computation, with corresponding ideal β-turns (see caption Fig. 8). Both, the turn NProO-modified L-proline at *i*+1 and the hydrazide "N"-retron mimicking glycine at *i*+2 display their equivalent backbone dihedrals Φ, Ψ in the same region of the Ramachandran plot as their parent natural amino acids.[41] **1** is seen as a versatile mimic of natural β-turns; ensemble conformer **1a** is a close mimic of type II and type I' β-turns. While in natural proteins, glycine at *i*+2 is frequently found in a type II turn configuration, type I' turns were shown to be effective hairpin inducers.[42]

In trying to rationalize the equilibrium ensemble composition of **1**, a comparison of hydrogen bonding in NXO-modified peptides with analog tetrapeptide turns composed of α-amino acids exclusively can be instructive.[43]At given temperature, pressure and concentration, the state of a small peptide in solution is characterized by the Boltzmann-weighted ensemble of molecular microstates, that is, a multitude of low-energy structures in dynamic equilibrium.[44] For a peptidomimetic, reproducing peptide secondary structure is an essential criterion; yet, in permitting technological application, the ability to represent the collectivity of ensemble properties is ultimately important.

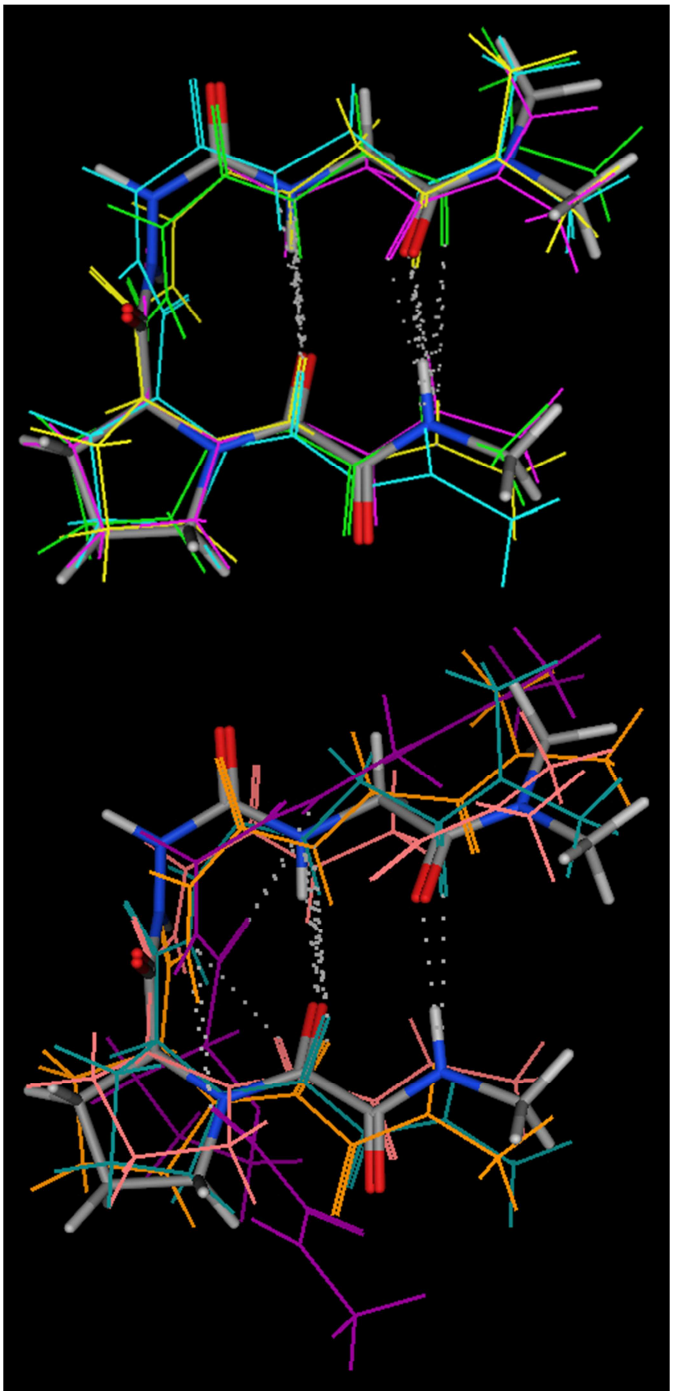

Fig. 8 Backbone RMSD-minimized superposition of the central MD conformer **1a** from MD simulations (OPLS-AA in water at 290K) with ideal turns. Ideal turn *i*+1 and *i*+2 torsions Φ, Ψ are taken from B. L. Sibanda, J. M. Thornton, *Nature* **1985**, *316*, 170. Turn types (model color, *i*+1 and *i*+2 backbone atom RMSD-difference to **1a** in Å): Upper model: I (green, 0.26); I' (yellow, 0.05); II (pink, 0.12); II' (turquoise, 0.25). Lower model: III (orange, 0.62); III' (seagreen, 0.11); V (amber, 0.16); V' (purple, 2.02). Dotted lines indicate hydrogen bonding.

Understanding of the long time observed conformational plurality manifested by β-sheets and the high mobility of β-strands due to inherent strand hydrogen bonding diversity was significantly advanced about a decade ago: Then, evidence was presented that in β-sheets, efficient cross-strand hydrogen bonding

requires a slightly "skewed" geometry with a relative register shift of opposite strands to minimize electrostatically repulsive interactions, concomitant factors of intrastrand hydrogen bonding.[45] These competing interactions cause the intrinsic conformational flexibility (in turn reflected by a shallow energy surface of Φ-torsions in the peptide backbone) of strands and, therefore, determine β-sheet ordering. This insight into β-structure conformational diversity led us to investigate whether it could be favorable to have an increased number of potential hydrogen bonding donor and acceptor moieties allocated in a peptidomimetic backbone. We envisaged a scenario of β-structure mimicry where, even in a polar medium like water, multiple hydrogen bonding capabilities constituted an asset rather than a liability.

To increase the number of potential interaction sites is advantageous from the perspective of statistical mechanics: Cross-strand hydrogen bond pairings that are laterally offset and hence inconsistent with formal sheet patterns are still entropically advantageous (and may "smear out" energetic separation between folded and completely unfolded states, the effect increasing with strand length). Structurally cooperative folding involving cross-strand backbone hydrogen bonding has been described before.[46] Given that the backbone modification meets the requirement of matching hydrogen bond donor and acceptor functions in a mutually attractive fashion (see Fig. 1), incorporation of a backbone donor/acceptor site manifold draws upon this effect. Then, since in a partially unfolded structure the contiguous placement of folded and unfolded strand sections was shown to be thermodynamically unfavorable,[47] presenting additional cross-strand hydrogen bonding options can drive the equilibrium towards folding by contributing positive entropy termini, diminishing the overall entropic cost of folding.[48] The free energy of folding for an ensemble species i at temperature T, ΔG_i, is given by

$$\Delta G_i = \Delta H_i - T\,\Delta S_i \qquad \text{Eq. (1)}$$

where H_i and S_i are the associated enthalpy and entropy of folding. S_i depends upon the measure of ensemble microstates Ω_i

$$S_i = k_B \ln \Omega_i \qquad \text{Eq. (2)}$$

where k_B is Boltzmann's constant. Ω_i relates the number of realized microstates n_i to the number of accessible microstates N_i

$$\Omega_i = N_i / n_i \qquad \text{Eq. (3)}$$

The relationship of Ω_i with ΔG_i is demonstrated for two folding ensemble entities, $i=j,k$. As simplifications, it is assumed that both species j,k attain the native fold and derive their entire stabilization from the same number of reversible, independent and isoenergetic interactions. Other contributions to entropy are neglected so that Eq. (2) represents the entire conformational entropy of the molecule. The intrinsic difference in free energy of folding between j,k can be expressed as

$$\Delta\Delta G_{jk} = \Delta\Delta H_{jk} - T\,(\Delta\Delta S_{jk}) \qquad \text{Eq. (4)}$$

The difference in the folding entropy term reads

$$\Delta\Delta S_{jk} = \Delta S_j - \Delta S_k = k_B \ln \Omega_j / \Omega_k = k_B (\ln \Omega_j - \ln \Omega_k) = k_B \Delta \ln \Omega_{jk} \qquad \text{Eq. (5)}$$

Further, with Eq. (3),

$$\Delta\Delta S_{jk} = k_B \left(\ln \frac{N_j}{n_j} - \ln \frac{N_k}{n_k} \right) = k_B \left(\Delta \ln N_{jk} - \Delta \ln n_{jk} \right) \qquad \text{Eq. (6)}$$

Thus, from entropy contributions alone and assuming $H_j=H_k$, the difference in folding free energy between species j,k is related to the difference in population of microstates ΔN_{jk} and Δn_{jk} by

$$\Delta\Delta G_{jk} = -k_B T \Delta \ln \Omega_{jk} = -k_B T \left(\Delta \ln N_{jk} - \Delta \ln n_{jk} \right) \qquad \text{Eq. (7)}$$

For $N_j > N_k$ and $n_j < n_k$, $\Delta\Delta G_{jk} < 0$. It is significant that both, a reduction in the number of accessible microstates N_k and an increase in the number of folded states n_k are fold-stabilizing species k relative to j. Whereas the favorability of reducing N_i (see Eq. (3)) is generally understood, foldamers exhibiting a plurality of interacting sites can capitalise on an increase of n_i to promote folding, as well.

In protein chemistry, the definition of higher-order structure is subject to rigorous characteristics. For structure classification, a set of formal criteria is consulted; structure elucidation focuses on the experimentally observable canonical ensemble member exclusively. Recently, facilitated by ever-increasing computing power, the analysis of protein dynamics has gained in importance. Significant advances in the understanding of ensemble dynamics and characterization of the molecular manifold have been made.[49] It is here that a foldamer-inspired outlook on peptidomimetics can view structure formation, dynamics and ordering from a different perspective: Structural energetics suggest that it is the dynamics of interconversion between folded, unfolded and partially folded states together with a rigidified potential energy surface of backbone torsions that guide the mimic when presenting the functionalities lined on it and relate closely to the performance of the mimic in attaining tight interaction profiles with molecular targets.[50] Consequently, RMSD difference as the criterion for comparing structure motifs gains in importance.

The folding event restructures a number of randomly ordered conformations through the formation of energetically stabilizing, non-covalent interactions. A reduction in the number of accessible ensemble conformations and accompanying loss of backbone and side chain conformational entropy is connected with a large energy penalty, known to be the single most unfavorable energetic factor in protein folding.[51] By virtue of strand-planarization through short-range dipole ordering its constituent "N"- and "O"-motifs, the NXO-modification enhances the interaction strength of both interstrand and solute-solvent hydrogen bonding, enthalpic factors contributing to a large negative ESF (Electrostatic Solvation Free Energy) upon folding.[52] Yet, incorporation of conformationally biased, "constrained" repeating motifs intrinsically predisposes the thermodynamic ensemble to undergo folding interactions. Likewise, decreasing accessibility to ensemble backbone conformations yields a lower conformational entropy penalty upon folding.[53]

The native state of **1** featuring two distinct folds **1a** and **1b** in equilibrium presents an opportunity to study the behavior of the NXO-modification in greater detail: It has been established that in absence of auxiliary stabilization, proline-*N cis* and *trans* amide isomers in proteins are nearly isoenergetic, the *cis* form usually being slightly disfavored.[54] The energetic barrier of roughly 20kcalmol^{-1} commonly associated with proline amide *cis*-

trans isomerizetion in proteins can be expected to be significantly lowered in a short peptide sequence.[55] Disregarding any further mechanism facilitating *cis-trans* isomerization (kinetics have been shown, *e.g.*, to be accelerated by intramolecular assistance via hydrogen bonding to a proline nitrogen acceptor, effectively enhancing the sp^3-character of the proline ring nitrogen and hence decreasing amide double bond resonance[56]), stabilization of the *cis*-proline fold **1b** can be rationalized from evaluation of the intrinsic energetics in the "O"-oxalamide retron: *Ab initio* quantum chemical energy profiling of relative configurations in oxalamides found the *all-trans* (*ttt*) conformer to be the minimum energy conformation in *N,N*'-dimethyloxalamide, with *cis-trans-trans* (*ctt*) and *cis-skew-cis* (*csc*) relatively destabilized by 6.2kcalmol^{-1} and 12.7kcalmol^{-1}, respectively.[57] In *csc*, an unfavorable steric interaction between the terminal NH-CH_3 in the methylamide and the preceding carbonyl was found, the distance being 2.82Å and thus slightly below the combined van der Waals radii.[58]

In **1**, the difference between *ttt* and *ctt* is lowered, the proline ring nitrogen being a tertiary amide. In the solvated minimum geometries from *ab initio* calculations (see Fig. 6), the hydrogen bonded oxalamide dihedrals N14-C15-C16-N17 are indeed seen arranged *skew* (145° and 137° for **1a** and **1b**, respectively). The "O"-retron in **1** attains *tst* and *csc* configuration; hence **1b** avoids an unfavorable steric clash of the terminal methyl C18 with C15(O) (in **1b**, the calculated distance C15(O)-C18 is 2.88 Å; the plane of the terminal methylamide, C16-N17-C18 is rotated 41° relative to the plane of C15-C16-O). Moreover, from Mulliken atomic charges, it was seen that upon hydration, the oxalamide carbonyls in *N,N*'-dimethyloxalamide become stronger H-bond acceptors (by -0.1 electrons); here, the much larger dipole moment of the *csc* minimum (3.07Debye in water) compared to both *ctt* and *ttt* (0.42 and ~0, respectively) allows for a stabilizing solvent-solute interaction, computed at 2.8kcalmol^{-1} relative to the global *ttt* minimum.[57a] These results suggest the "O"-retron in **1** to gain upon stabilization through intrastrand hydrogen bonding; however, in **1b**, this interaction can only be realized with the methyloxalamide unit in *cis* configuration at C16-N17. Taken together, this arrangement then satisfies a *skew* oxalyl unit at C15-C16 and a second (C3(O)←HN17) hydrogen bond, at the cost of a further insignificant *cis* amide energy penalty.

3 Conclusions

In summary, employing NXO-peptidomimicry, we have created a minimal β-sheet increment featuring the N^LProO-modification as novel β-hairpin nucleator. Simulation and spectroscopy account for folding to a turn/hairpin native state in polar solvents, including water, at room temperature. Thus, even in a minimal tetrapeptide mimic, NXO can impart β-structure characteristics and achieve secondary structure mimicry. As an outlook towards further studies, the high designability and ready diversification, together with excellent solubility properties in polar media, render NXO-derived β-structures valuable scaffolds for the elaboration of β-peptidomimetics in water.

Notes and references

[a] Integrative Regenerative Medicine Centre (IGEN) & Department of Physics, Chemistry and Biology (IFM), Linköping University Campus Valla, 58183 Linköping (Sweden). E-mail: jayph@ifm.liu.se

[b] Institute of Applied Synthetic Chemistry, Vienna University of Technology, Getreidemarkt 9/163, A-1060 Vienna (Austria).

[c] Department of Environmental Geosciences, University of Vienna, Althanstrasse 14, A-1090 Vienna (Austria).

[d] Department of NMR and Mass Spectrometry, Institute of Analytical Chemistry, Faculty of Chemical and Food Technology, Slovak University of Technology, Radlinského 9, 81237 Bratislava (Slovak Republic).

[e] Department of Physical Chemistry, University of Plovdiv, Tzar Assen Street 24, 4000 Plovdiv (Bulgaria)

† Electronic Supplementary Information (ESI) available: Experimental details of Synthesis and characterization details, Mass, NMR, CD spectra, computational data. See DOI: 10.1039/b000000x/

1 For an overview, see: a) *Synthesis of peptidomimetics in Houben-Weyl Methods of Organic Chemistry*, ed. M. Goodman, A. Felix, L. Moroder, C. Toniolo, Thieme, Stuttgart, Germany, 2003**,** Vol. E22c, See in particular b) M. Kahn, M. Eguchi, *Synthesis of peptides incorporating β-turn inducers and mimetics*, Vol. E22c, ch. 12.1, pp. 695, and c) P. Chitnumsub, S. Deechongkit, R. Kaul, J. P. Schneider, K. Y. Tsang, A. Moretto, H. Bekele, S. R. LaBrenz, H. A. Lashuel, J. W. Kelly, *Synthesis of β-sheet peptides and proteins incorporating templates*, Vol. E22c, ch. 12.4, pp. 793. For a research spotlight, see d) Y-D. Wu and S. Gellman, *Acc. Chem. Res.*, 2008, **41**, 1231; Further: e) M. G. Hinds, N. G. Richards, J. A. Robinson, *J. Chem. Soc. Chem. Comm.*, 1988, **22**, 1447; f) W. C. Ripka, G. V. De Lucca, A. C. Bach II, R. S. Pottorf, J. M. Blaney, *Tetrahedron*, 1993, **49**, 3593; For selected reviews, see g) W. A. Loughlin, J. D. A. Tyndall, M. P. Glenn, D. P. Fairlie, *Chem. Rev.*, 2004, **104**, 6085; see also update 1, *Chem. Rev*., 2010, **110**, PR32-69; h) J. D. A. Tyndall, B. Pfeiffer, G. Abbenante, D. P. Fairlie, *Chem. Rev.*, 2005, **105**, 793; see also update 1, *Chem. Rev*., 2010, **11**, PR1-PR41; i) J. Venkatraman, S. C. Shankaramma, P. Balaram, *Chem. Rev*., 2001, **101**, 3131; j) D. J. Hill, M. J. Mio, R. B. Prince, T. S. Hughes, J. S. Moore, *Chem. Rev*., 2001, **101**, 3893; k) R. P. Cheng, S. H. Gellman, W. F. DeGrado, *Chem. Rev.*, 2001, **101**, 3219; l) A. Grauer, B. Koenig, *Eur. J. Org. Chem.*, 2009, **30**, 5099; m) T. A. Martinek, F. Fueloep, *Chem. Soc. Rev*., 2012, **41**, 687; n) W. S. Horne, *Expert Opin. Drug Dis.* **2011**, *6*, 1247; o) G. Licini, L. J. Prins, P. Scrimin, *Eur. J. Org. Chem.*, 2005, **6**, 969; p) A. G. Jamieson, N. Boutard, D. Sabatino, W. D. Lubell, *Chem. Biol. Drug Des.*, 2013, **81**, 148; q) S. Mallakpour, M. Dinari, *J. Macromol. Sci. A*, 2011, **48**, 644; r) R. M. J. Liskamp, D. T. S. Rijkers, J. A. W. Kruijtzer, J. Kemmink, *ChemBioChem*, 2011, **12**, 1626; s) G. Guichard, I. Huc, *Chem. Comm.*, 2011, **47**, 5933; t) C. M. Goodman, S. Choi, S. Shandler, W. F. DeGrado, *Nat. Chem. Biol.*, 2007, **3**, 252; u) B. C. Gorske, J. R. Stringer, B. L. Bastian, S. A. Fowler, H. E. Blackwell, *J. Am. Chem. Soc.*, 2009, **131**, 16555.

2 a) C. K. Smith, L. Regan, *Acc. Chem. Res.*, 1997, **30**, 153; b) J. S. Merkel, J. M. Sturtevant, L. Regan, *Structure*, 1999, ***7***, 1333; c) E. G. Hutchinson, R. B. Sessions, J. M. Thornton, D. N. Woolfson, *Pro. Sci.*, 1998, **7**, 2287.

3 a) C. K. Smith, J. M. Withka, L. Regan, *Biochemistry*, 1994, **33**, 5510; b) R. M. Hughes, M. L. Waters, C*urr. Op. Struct. Biol.*, 2006, **16**, 514; c) H. M. Fooks, A. C. R. Martin, D. N. Woolfson, R. B. Sessions, E. G. Hutchinson, *J. Mol. Biol.*, 2006, **356**, 32.

4 a) U. Jordis, J. Phopase, *PCT Int. Appl.*, WO2007095980, 2007; b) J. B. Phopase, Ph.D. Thesis, Vienna University of Technology, 2008.

5 C. Rabong, U. Jordis, J. B. Phopase, *J. Org. Chem.*, 2010, **75**, 2492.

6 G. N. Ramachandran, C. Ramakrishnan, V. Sasisekharan, *J. Mol. Biol.*, 1963, **7**, 95; see also Ref. 5.

7 a) T. Moriuchi, T. Hirao, *Chem. Soc. Rev.*, 2004, **33**, 294; b) H. Diaz, K. Y. Tsang, D. Choo, J. W. Kelly, *Tetrahedron*, 1993, **49**, 3533; c) W. M. De Borggraeve, F. J. R. Rombouts, E. V. Van der Eycken, S. M. Toppet, G. J. Hoornaert, *Tet. Lett.*, 2001, **42**, 5693; d) Y. Krishnan -Ghosh, S. Balasubramanian, *Angew. Chem.*, 2003, **115**, 2221; *Angew. Chem. Intl. Ed.*, 2003, **42**, 2171; e) Y. Angell, D. Chen, F. Brahimi, H. U. Saragovi, K. Burgess, *J. Am. Chem. Soc.*, 2008, **130**, 556; f) A. A. Fuller, D. Du, F. Liu, J. E. Davoren, G. Bhabha, G. Kroon, D. A. Case, H. J. Dyson, E. T. Powers, P. Wip, et al. *Proc. Natl. Acad. Sci. U.S.A.*, 2009, **106**, 11067.

8 a) R. L. Baldwin, *J. Biol. Chem.*, 2003, **278**, 17581; b) E. S. Eberhardt, R. T. Raines, *J. Am. Chem. Soc*., 1994, **116**, 2149; c) C. Park, M. J. Carlson, W. A. Goddard III, *J. Phys. Chem. A*, 2000, **104**, 2498; d) J. D. Fisk, S. H. Gellman, *J. Am. Chem. Soc*., 2001, **123**, 343; e) J. M. Langenhan, S. H. Gellman, *Org. Lett.*, 2004, **6**, 937; f) J. D. Fisk, M. A. Schmitt, S. H. Gellman, *J. Am. Chem. Soc.*, 2006, **128**, 7148; g) L. Eidenschink, B. L. Kier, K. N. L. Huggins, N. H. Andersen, *Proteins*, 2009, **75**, 308.

9 a) S. Albeck, R. Unger, G. Schreiber, *J. Mol. Biol.*, 2000, **298**, 503; b) M. S. J. Searle, *Chem. Soc., Perk. T. 2*, 2001, 1011; c) H.-J. Schneider, *Angew. Chem.*, 2009, **121**, 3982; *Angew. Chem. Intl. Ed.*, 2009, **48**, 3924.

10 yyyy a) K. Dill, *Biochemistry* **1990**, *29*, 7133; b) S. Deechongkit, H. Nguyen, E. T. Powers, P. E. Dawson, M. Gruebele, J. W. Kelly, *Nature* **2004**, *430*, 101.

11 yyyy M. Jager, S. Deechongkit, E. K. Koepf, J. Nguyen, J. Gao, E. T. Powers, M. Gruebele, J. W. Kelly, *Peptide Sci*. **2008**, *90*, 751, and references cited therein.

12 a) Y. Che, G. R. Marshall, *J. Med. Chem.*, 2006, **49**, 111; b) M. Hosoya, Y. Otani, M. Kawahata, K. Yamaguchi, T. Ohwada, *J. Am. Chem. Soc*., 2010, **132**, 14780. See also Refs. 1d and 7d.

13 a) K. S. Rotondi, L. M. Gierasch, *Biopolymers*, 2006, **84**, 1; b) W. J. Cooper, M. L. Waters, *Org. Lett.*, 2005, **7**, 3825; c) U. Arnold, B. R. Huck, S. H. Gellman, R. T. Raines, *Protein Sci.*, 2013, **22**, 274; d) S. Deechongkit, H. Nguyen, H.; M. Jager, E. T. Powers, M. Gruebele, J. W. Kelly, *Curr. Op. Struct. Biol.*, 2006, **16**, 94. See also Refs. 1e and 7f.

14 P. Y. Chou, G. D. Fasman, *J. Mol. Biol.*, 1977, **115**, 135.

15 a) W. Maison in *Highlights in Bioorganic Chemistry*, (Eds.: C. Schmuck, H. Wennemers), Wiley-VCH: Weinheim, Germany, 2004, pp. 18; b) Cheng, R. P. *Curr. Op. Struct. Biol.*, 2004, **14**, 512.

16 a) K. Möhle, M. Gassmann, H.-J. Hofmann, *J. Comput. Chem.*, 1997, **18**, 1415; b) M. H. V. R. Rao, S. K. Kumar, A. C. Kunwar, *Tet. Lett.*, 2003, **44**, 7369; c) J. L. Baeza, G. Gerona-Navarro, M. J. Perez de Vega, M. T. Garcia-Lopez, R. Gonzalez-Muniz, M. Martin-Martinez, *J. Org. Chem.*, 2008, **73**, 1704.

17 a) F. Blanco, M. Ramirez-Alvarado, L. Serrano, *Curr. Op. Struct. Biol.*, 1998, **8**, 107; b) S. H. Gellman, *Curr. Op. Struct. Biol*., 1998, **2**, 717.

18 a) S. M. Cowell, Y. S. Lee, J. P. Cain, V. J. Hruby, *Curr. Med. Chem.*, 2004, **11**, 2785; b) T. Hayashi, T. Asai, H. Ogoshi, *Tet. Lett.*, 1997, **38**, 3039; c) P. Cristau, M.-T. Martin, M.-E. T. H. Dau, J.-P. Vors, J. Zhu, *Org. Lett.*, 2004, **6**, 3183; d) J. V. Sponer, J. Leszczynski, P. Hobza, *J. Mol. Struct.-Theochem*, 2001, **573**, 43; e) C. Mothes, M. Larregola, J. Quancard, N. Goasdoue, S. Lavielle, G. Chassaing, O. Lequin, P. Karoyan, *ChemBioChem*, 2010, **11**, 55; f) H.-J. Lee, K.-H. Choi, I.-A. Ahn, S. Ro, H. G. Jang, Y.-S. Choi, K.-B. Lee, *J. Mol. Struct.-Theochem*, 2001, ***569***, 43.

19 Compare: a) A. Aubry, J. P. Mangeot, J. Vidal, A. Collet, S. Zerkout, M. Marraud, *Int. J. Pept. Prot. Res.*, 1994, **43**, 305; b) L. Halab, J. A. J. Becker, Z. Darula, D. Tourwe, B. L. Kieffer, F. Simonin, W. D. Lubell, *J. Med. Chem.*, 2002, **45**, 5353; c) M. Krasavin, V. Parchinsky, A. Shumsky, I. Konstantinov, A. Vantskul, *Tet. Lett.*, 2010, **51**, 1367.

20 D. Ranganathan, *Pure Appl. Chem.*, 1996, **68**, 671.

21 Compare: a) X. Daura, K. Gademann, H. Schaefer, B. Jaun, D. Seebach, W. F. van Gunsteren, *J. Am. Chem. Soc.* 2001, **123**, 2393; b) C. M. Santiveri, M. A. Jimenez, M. Rico, W. F. van Gunsteren, X. Daura, *J. Pept. Sci.*, 2004, **10**, 546.

22 W. L. Jorgensen, D. S. Maxwell, J. Tirado-Rives, *J. Am. Chem. Soc.*, 1996, **117**, 11225. See also previous modeling of an NXO-peptide in Ref. 5.

23 a) C. M. Venkatachalam, *Biopolymers*, 1968, **6**, 1425; b) B. L. Sibanda, T. L. Blundell, J. M. Thornton, *J. Mol. Biol.*, 1989, **206**, 759; see also Ref. 17b.

24 G. D. Rose, L. M. Gierasch, J. A. Smith, *Adv. Protein Chem.*, 1985, **37**, 1.

25 E. J. Milner-White, B. M. Ross, R. Ismail, K. Belhadj-Mostefa, R. Poet, *J. Mol. Biol.*, 1988, **204**, 777.

26 S. K. Awasthi, S. Raghothama, P. Balaram, *Biochem. and Biophys. Res. Comm.*, 1995, **216**, 375; see also Refs. 18b and 18f.

27 See Ref. 6; see also S. C. Lovell, I. W. Davis, W. B. Arendall III; P. I. W. de Bakker, J. M. Word, M. G. Prisant, J. S. Richardson, D. C. Richardson, *Proteins*, 2003, **50**, 437.

28 a) J. M. Word, S. C. Lovell, T. H. LaBean, H. C. Taylor, M. E. Zalis, B. K. Presley, J. S. Richardson, D. C. Richardson, *J. Mol. Biol.*, 1999, **285**, 1711; b) B. K. Ho, A. Thomas, R. Brasseur, *Pro. Sci.*, 2003, **12**, 2508; a minor peak sampling Ψ around -50° in the α-region and corresponding to the opened fold was observed, as well; see Figure 5 supplementary information.

29 a) B. K. Ho, R. Brasseur, *BMC Struct. Biol.*, 2005, **5**, 14: b) M. Thormann, H.-J. Hofmann, *J. Mol. Struct-Theochem*, 1999, **469**, 63.

30 R. Guenther, H.-J. Hofmann, *J. Am. Chem. Soc.*, 2001, **123**, 247.

31 Formation of the γ-turn relative minimum conformer was calculated to be slightly exergonic with ΔG^0_{298}=-0.7±0.3kcalmol^{-1}, at the B3LYP/6-311G++(d,p) level of theory, using solvation SCRF=water in the GAUSSIAN program package (M. J. Frisch, G. W. Trucks, H. B. Schlegel, G. E. Scuseria, M. A. Robb, J. R. Cheeseman, G. Scalmani, V. Barone, B. Mennucci, G. A. Petersson, et al., *Gaussian 09*, Revision A.01, Gaussian, Inc., Wallingford CT, **2009**). Relative to the extended conformation, the native fold exhibiting the γ-turn motif realizes energetic stabilization overtly from van der Waals (-2.4 ±0.5kcalmol^{-1}) and electrostatic termini (-6±1kcalmol^{-1}; from a 100ns MD trajectory in water at 290K; see Table 2, supplementary information). Compare C. Guo, H. Levine, D. A. Kessler, *Phys. Rev. Lett.*, 2000, **84**, 3490.

32 The conformation with an extended backbone typically samples the hydrazide dihedral H-N7-N8-H around -120°, whereas in the fold **1** this angle is typically seen around +110°; thus, the relative popula-

tions of this torsion also reflect the population of the corresponding conformers (see Figures 2-4, supplementary information).

33 J. S. Nowick, D. M. Chung, K. Maitra, S. Maitra, K. D. Stigers, Y. Sun, *J. Am. Chem. Soc.*, 2000, **122**, 7654.

34 K. Scott, J. Stonehouse, J. Keeler, A. J. Shaka, *J. Am. Chem. Soc.*, 1995, **117**, 4199.

35 For a recent general review, see: J. R. Allison, *Biophys. Rev*., 2012, **4**, 189.

36 G. Fischer, *Angew. Chem.*, 1994, **106**, 1479; *Angew. Chem. Intl. Ed.*, 1994, **33**, 1415.

37 From calculated potential energies with SCRF=water solvation, at B3LYP with the 6-311G++(d,p) basis set. It is seen that isomer **1b** gains stabilization of 1.3kcalmol^{-1} relative to **1a** upon solvation from vacuum; see supplementary information for details.

38 The backbone dihedrals for **1b** are, from the *ab initio* calculated lowest energy conformer, at *i*+1: Φ=-73°, Ψ=+131°; at *i*+2 Φ =+92°, Ψ=+21°.

39 a) R. W. Woody, *Circular Dichroism, in: Houben-Weyl Methods of Organic Chemistry*, *Vol.* **E22b**, *Chapter 7.7.3* (Eds.: M. Goodman, A. Felix, L. Moroder, C. Toniolo), Thieme: Stuttgart, Germany, 2003, pp. 739; b) E. Lacroix, T. Kortemme, M. L. De la Paz, L. Serrano, *Curr. Op. Struct. Biol.*, 1999, **9**, 487; c) R. W. Driver, H. N. Hoang, G. Abbenante, D. P. Fairlie, *Org. Lett.*, 2009, **11**, 3092; d) R. S. Harrison, N. E. Shepherd, H. N. Hoang, G. Ruiz-Gomez, T. A. Hill, R. W. Driver, V. S. Desai, P. R. Young, G. Abbenante, D. P. Fairlie, *Proc. Natl. Acad. Sci. U.S.A.*, 2010, **107**, 11686.

40 a) H. Diaz, K. Y. Tsang, D. Choo, J. W. Kelly, *Tetrahedron*, 1993, **49**, 3533; b) K. H. Mayo, E. Ilyina, H. Park, *Pro. Sci.*, 1996, **5**, 1301; c) T. Mori, S. Yasutake, H. Inoue, K. Minagawa, M. Tanaka, T. Niidome, Y. Katayama, *Biomacromolecules*, 2007, **8**, 318; see also Refs. 23a and 39c.

41 Comparison of backbone-RMSD from the superposition of molecular fragments consisting of different constituent atoms as in Fig. 8 appears yet justified given the backbone pitch (measured as the distance between sequential α-carbons) in NXO-modified peptides being close to natural peptide sequences: For example, *ab initio* calculations gave the pitch between equivalent backbone atoms in a truncated NAlaO pseudopeptide, MeNHCO-N^{L}AlaO-NHMe, at 7.44±0.04Å, deviating less than 1.8% from the distance in a corresponding sheet like L-alanine tripeptide, the latter calculated at 7.57±0.04Å for the distance between the terminal α-carbons.

42 a) H. E. Stanger, S. H. Gellman, *J. Am. Chem. Soc.*, 1998, **120**, 4236, and references cited therein; b) R. R. Gardner, G.-B. Liang, S. H. Gellman, *J. Am. Chem. Soc.*, 1999, **121**, 1806; c) K. Gunasekaran, C. Ramakrishnan, P. Balaram, *Prot. Eng*, 1997, **10**, 1131; for more recent examples of exploiting type-I β-turns, see d) M. D. Mukrasch, P. Markwick, J. Biernat, M. Von Bergen, P. Bernado, C. Griesinger, E. Mandelkow, M. Zweckstetter, M. Blackledge, *J. Am. Chem. Soc.*, 2007, **129**, 5235; e) B. Bulic, M. Pickhardt, B. Schmidt, E.-M. Mandelkow, H. Waldmann, E. Mandelkow, *Angew. Chem.*, 2009, **121**, 1772; *Angew. Chem. Intl. Ed.*, 2009, **48**, 1740.

43 a) E. A. Archer, H. Gong, M. J. Krische, *Tetrahedron*, 2001, **57**, 1139; b) F. Avbelj, R. L. Baldwin, *Proc. Natl. Acad. Sci. U.S.A.*, 2004, 101, 10967.

44 K. Makabe, S. Yan, V. Tereshko, G. Gawlak, S. Koide, *J. Am. Chem. Soc*., 2007, **129**, 14661.

45 a) I. L. Shamovsky, G. M. Ross, R. J. Riopelle, *J. Phys. Chem. B*, 2000, **104**, 11296 and references cited therein; b) B. K. Ho, P. M. G. Curmi, *J. Mol. Biol.*, 2002, **37**, 291; c) J. Rossmeisl, B. Hinnemann, K. W. Jacobsen, J. K. Norskov, O. H. Olsen, J. T. Pedersen, *J. Chem. Phys.*, 2003, **118**, 9783; d) P. Bour, T. A. Keiderling, *J. Mol. Struct.-Theochem*, 2004, ***675***, 95; e) S. Scheiner, *J. Phys. Chem. B*, 2007, **111**, 11312.

46 a) V. J. Hilser, D. Dowdy, T. G. Oas, E. Freire, *Proc. Natl. Acad. Sci. U.S.A.*, 1998, **95**, 9903; b) C. Guo, M. S. Cheung, H. Levine, D. A. Kessler, *J. Chem. Phys*., 2002, **116**, 4353; c) J. Rossmeisl, J. K. Norskov, K. W. Jacobsen, *J. Am. Chem. Soc*., 2004, **126**, 13140; d) D. R. Roe, V. Hornak, C. Simmerling, *J. Mol. Biol*., 2005, **352**, 370; e) E. Koh, T.. Kim, H. Cho, *Bioinformatics*, 2006, **22**, 297; f) V. Munoz, R. Ghirlando, F. J. Blanco, G. S. Jas, J. Hofrichter, W. A. Eaton, *Biochemistry*, 2006, **45**, 7023; g) T. Yoda, Y. Sugita, Y. Okamoto, *Proteins*, 2007, **66**, 846.

47 C. Guo, H. Levine, D. A. Kessler, *Proc. Natl. Acad. Sci. U.S.A.*, 2000, **97**, 10775.

48 Compare: a) Y.-L. Zhao, Y.-D. Wu, *J. Am. Chem. Soc*., 2002, **124**, 1570; b) D. W. Bolen, G. D. Rose, *Annu. Rev. Biochem.*, 2008, **77**, 339.

49 a) V. J. Hilser, B. García-Moreno E., T. G. Oas, G. Kapp, S. T. Whitten, *Chem. Rev.*, 2006, **106**, 1545; b) M. C. Baxa, E. J. Haddadian, A. K. Jha, K. F. Freed, T. S. Sosnick, *J. Am. Chem. Soc.*, 2012, **134**, 15929.

50 See Ref. 11; for selected reviews, see: a) H. Gohlke, G. Klebe, *Angew. Chem.*, 2002, **114**, 2764; *Angew. Chem. Intl. Ed.*, 2002, **41**, 2644; b) K. N. Houk, A. G. Leach, S. P. Kim, X. Zhang, *Angew. Chem.*, 2003, **115**, 5020; *Angew. Chem. Intl. Ed.*, 2003, **42**, 4872. See also S. P. Edgcomb, K. P. Murphy, *Curr. Op. Biotech*., 2000, **11**, 62.

51 It has been noted that the largest contribution to the free energy of folding came from stabilization through backbone hydrogen bonding and not from side chain interactions, see Ref. 8a and references cited therein; see also Ref. 43b and C. Zhang, J. L. Cornette, C. Delisi, *Pro. Sci.*, 1997, **6**, 1057.

52 R. L. Baldwin, *J. Mol. Biol.*, 2007, **371**, 283.

53 J. A. D'Aquino, J. Gómez, V. J. Hilser, K. H. Lee, L. M. Amzel, E. Freire, *Proteins*, 1996, **25**, 143.

54 a) W. J. Wedemeyer, E. Welker, H. A. Scheraga, *Biochemistry*, 2002, **41**, 14637; b) Y. K. Kang, *J. Phys. Chem. B*, 2002, **106**, 2074; c) G. Fischer, *Chem. Soc. Rev*., 2000, **29**, 119.

55 C. Dugave, L. Demange, *Chem. Rev*., 2003, **103**, 2475.

56 a) S. Fischer, R. L. Dunbrack Jr., M. Karplus, *J. Am. Chem. Soc*., 1994, **116**, 11931; b) C. Cox, T. Lectka, *J. Am. Chem. Soc.*, 1998, **120**, 10660; c) O. E. Schroeder, E. Carper, J. W. Wind, J. L. Poutsma, F. A. Etzkorn, J. C. Poutsma, *J. Phys. Chem. A*, 2006, **110**, 6522.

57 a) C. Aleman, J. Puiggali, *J. Org. Chem.*, 1999, **64**, 351. Compare also b) S. Ahn, F. Guo, M. K. Benson, K. D. M. Harris, *J. Am. Chem. Soc*., 2006, **128**, 8441.

58 For *N,N*'-diacetylhydrazide, the *trans-gauche-trans* (*tgt*) isomer was found the most stable, with *ttt* and *cgt* being 1.3kcalmol^{-1} and 1.4kcalmol^{-1} less stable, respectively. The NH-bond was again seen relatively deshielded (by +0.05 electrons) upon hydration; see Ref. 57a and compare analysis of the hydrazide "N"-retron above, chapter 2.2.

Table of content

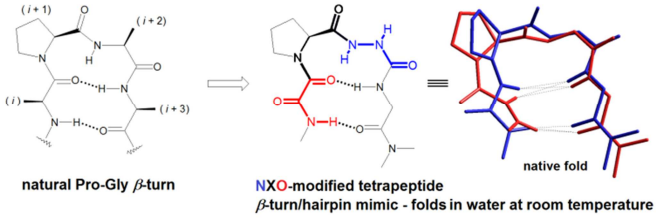

Incorporating the proline-derived NProO peptidomimetic building block, a minimal tetrapeptide β-turn/hairpin mimic is shown to emulate a natural proline-glycine β-turn in polar medium, including water at room temperature.

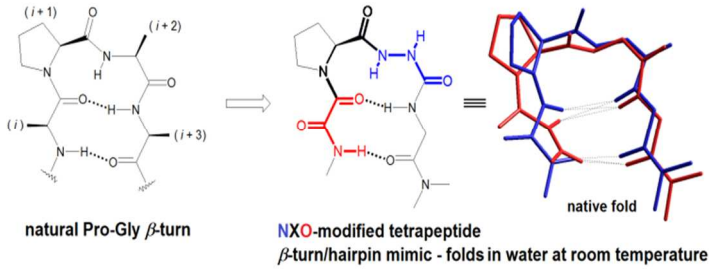

NXO building block derived minimal tetrapeptide emulate the natural proline-glycine β-turn/hairpin in polar medium, including water at room temperature.